Annals of Botany **125**: 785–803, 2020
doi: 10.1093/aob/mcz158, available online at www.academic.oup.com/aob

ANNALS OF BOTANY
Founded 1887

PART OF THE FOCUS ISSUE ON PLANT DEFENCE AND STRESS REPSONSE

Overexpression of *PtHMGR* enhances drought and salt tolerance of poplar

Hui Wei[1,†], Ali Movahedi[1,†], Chen Xu[1,2,†], Weibo Sun[1,†], Lingling Li[1], PuWang[1], Dawei Li[1] and Qiang Zhuge[1,*]

[1]Key Laboratory of Forest Genetics & Biotechnology of Ministry of Education, Co-Innovation Center for Sustainable Forestry in Southern China, College of Biology and the Environment, Nanjing Forestry University, Nanjing 210037, China and [2]Jiangsu Provincial Key Construction Laboratory of Special Biomass Resource Utilization, Nanjing Xiaozhuang University, Nanjing 211171, China
**For correspondence. E-mail qzhuge@njfu.edu.cn*
[†]Equal first authors.

Received: 25 April 2019 Returned for revision: 20 August 2019 Editorial decision: 24 September 2019 Accepted: 28 September 2019
Published electronically 2 October 2019

• **Background and Aims** Soil salinization and aridification are swiftly engulfing the limited land resources on which humans depend, restricting agricultural production. Hydroxy-3-methylglutaryl coenzyme A reductase (HMGR) is important in the biosynthesis of terpenoids, which are involved in plant growth, development and responses to environmental stresses. This study aimed to provide guidance for producing salt- and drought-resistant poplar.
• **Methods** A protein expression system was used to obtain PtHMGR protein, and high-performance liquid chromatography was used to detect the activity of PtHMGR protein *in vitro*. In addition, a simplified version of the leaf infection method was used for transformation of 'Nanlin895' poplar (*Populus* × *euramericana*). qRT–PCR was used to identify expression levels of genes.
• **Key Results** PtHMGR catalysed a reaction involving HMG-CoA and NADPH to form mevalonate. Overexpression of *PtHMGR* in *Populus* × *euramericana* 'Nanlin895' improved drought and salinity tolerance. In the presence of NaCl and PEG_{6000}, the rates of rooting and survival of *PtHMGR*-overexpressing poplars were higher than those of wild-type poplars. The transgenic lines also exhibited higher proline content and peroxidase and superoxide dismutase activities, and a lower malondialdehyde level under osmotic stress. In addition, the expression of genes related to reactive oxygen species (ROS) scavenging and formation was altered by osmotic stress. Moreover, the effect of osmotic stress on transcript levels of stress-related genes differed between the transgenic and wild-type poplars.
• **Conclusion** PtHMGR catalysed a reaction involving HMG-CoA and NADPH to form mevalonate *in vitro*. Overexpression of *PtHMGR* promoted root development, increased the expression of ROS scavenging-related genes, decreased the expression of ROS formation-related genes, and increased the activity of antioxidant enzymes in transgenic poplars, enhancing their tolerance of osmotic stress. In addition, overexpression of *PtHMGR* increased expression of the stress-related genes *KIN1*, *COR15* and *AAO3* and decreased that of *ABI*, *MYB*, *MYC2* and *RD22*, enhancing the stress resistance of poplar.

Key Words: *HMGR*, terpenoids, *Populus trichocarpa*, drought tolerance, salinity tolerance, ROS.

INTRODUCTION

Plant secondary metabolism is the result of the interaction of plants with the environment. Secondary metabolites play an important role in the self-protection, survival and competitiveness of plants and coordinate their interactions with the surrounding environment. Compounds consisting of isoprene units and their derivatives are the most widely distributed and complex secondary metabolites in nature (Markus *et al*., 2000; Yonekura *et al*., 2009). Many isoprene compounds participate in the physiological activities of organisms and the synthesis of pigments during plant growth and development. Plant hormones regulate growth, development and defence against biotic and abiotic stresses (Wu *et al.*, 1997). For example, abiotic stress responses are relevant to the production of reactive oxygen species (ROS) in plant cells. Volatile isoprenoids can alleviate the effects of oxidative stress by regulating the oxidative state of plants (Vickers *et al.*, 2009). Volatile isoprenoids can also alleviate oxidation and thermal stress in plants and promote both direct and indirect defence by regulating signals of the biochemical activation of defence pathways (Loreta and Schnitzler, 2010). In addition, carbon is allocated to stress-induced volatile compounds, which play a significant role in protecting plants from abiotic stresses (Mithöfer and Boland, 2012; Loreto *et al.*, 2014) In plants, terpenoids are synthesized by the methylerythritol phosphate (MEP) and mevalonate pathways (Yu and Utsumi, 2009). Based on their locations, the mevalonate pathway is known as the cytoplasmic pathway and the MEP pathway as the plastid pathway (Estevez *et al.*, 2001). The mevalonate and MEP pathways also synthesize isopentenyl diphosphate (IPP) and dimethylallyl diphosphate (DMAPP) precursors, as well as the terpenoids required for growth and development (Schwender *et al.*, 2001; Miziorko, 2011). Hydroxy-3-methylglutaryl coenzyme A reductase (HMGR) is the first and rate-limiting enzyme in the mevalonate metabolic pathway and catalyses the reaction

of 3-hydroxy-3-methyl-glutaric coenzyme A (HMG-CoA) with NADPH to produce the intermediate metabolite methyl valerate. The synthesis of IPP and its allylic isomer DMAPP is the first step in both the mevalonate and the MEP pathway (Maldonado *et al*., 1992). The mevalonate pathway is responsible for producing sesquiterpenoids, sterols and secondary triterpenes (Leivar *et al.*, 2011), whereas the MEP pathway is primarily responsible for synthesis of monoterpenoids, diterpenoids, essential photosynthesis pigments and plastidial quinones. Plants have two ABA (as a sesquiterpene compound) synthesis pathways; the indirect pathway is responsible for the production of most ABA. 9-*Cis*-epoxy carotenoid dioxygenase (NCED) is a rate-limiting factor in the biosynthesis of ABA (Finkelstein, 2013). In plants, the *NCED* expression level is positively correlated with ABA content (Christmann *et al.*, 2005). Higher plants under stress have an increased endogenous ABA content, resulting in a series of responses, e.g. solute outflow and stomatal closure of guard cells. ABA has the most significant response to drought and salt stress (Chaves *et al.*, 2003). In addition, the increased ABA content of plants under osmotic stress results in upregulation of various downstream genes, e.g. *P5CS* (Székely *et al.*, 2008) and *KIN1* (Xiong *et al.*, 2002). Environmental changes can suppress plant growth and development (Ahuja *et al.*, 2010). Abiotic stresses include drought, high temperature, low temperature, nutrient deprivation, excessive salt and heavy metals. Drought, salt and temperature stresses affect the geographical distribution of plants and limit agricultural yields. Plants perceive abiotic stresses through specific sensors and in response alter their growth, metabolism and development (Ahuja *et al.*, 2010). Therefore, improving the stress tolerance of plants is critical for enhancing agricultural yields and for environmental sustainability. Poplar is an economically important forest tree species that grows in temperate and cold-temperate regions of the northern hemisphere. Also, poplar as a model woody plant has been widely used in scientific research since the announcement of the poplar genome (Tuskan *et al.*, 2006), and genetic engineering has often been used to modify poplars for adaptation to a variety of environments. However, the characterization and function of *HMGR* of *Populus trichocarpa*, which codes for the rate-limiting enzyme, has remained unclear. Research on poplar HMGR would enhance our understanding of the mevalonate and MEP pathways and facilitate forest-tree breeding programmes. In this study we cloned *HMGR* of *P. trichocarpa* and analysed the structure and function of HMGR. We also analysed *PtHMGR* expression in plant parts and the effect of abiotic stresses on its expression. In addition, we evaluated the effect of *PtHMGR* overexpression on plant antioxidant levels and the expression of osmotic stress-related genes and of genes related to the ABA-mediated response to osmotic stress. These data enhance our understanding of PtHMGR function and provide us with a theoretical basis for genetic improvement of poplar.

MATERIALS AND METHODS

Plant materials and treatments

Populus trichocarpa and *Populus* × *euramericana* 'Nanlin895' were cultured in half-strength Murashige and Skoog (MS) medium under a 16 h light/8 h dark cycle at 23 °C and 74 % humidity. *Populus trichocarpa* seedlings were subcultured after 1 month for an additional 1 month. Subsequently, *P. trichocarpa* seedlings were treated with 200 μM ABA, 200 μM salicylic acid (SA), 200 μM jasmonic acid (JA), 2 mM hydrogen peroxide (H_2O_2), 200 mM NaCl or 10 % PEG_{6000}. Total RNA was extracted from samples using the Plant Mini RNA Kit (TaKaRa, Japan).

Cloning of PtHMGR and bioinformatics analysis

The MMLV reverse transcriptase and forward and reverse primers (Supplementary Data Table S1) were used to amplify cDNA using poly(A)-enriched mRNA from leaves and the open reading frame (ORF) of *PtHMGR*. The PCR system was as follows: 2.0 μL cDNA as template, 2 μL forward and reverse primers (10 μmol), 1 μL dNTPs (10 mM), 5.0 μL 10× PCR buffer (Mg^{2+} plus), 0.5 μL rTaq DNA polymerase (Takara, Japan) and 38.5 μL ddH_2O. The PCR procedure was as follows: 95 °C for 10 min; 35 cycles of 95 °C for 2 min, 56 °C for 2 min and 72 °C for 2 min; and finally 72 °C for 10 min. We amplified the 5′ and 3′ UTR regions by RACE PCR with specific primers (Supplementary Data Table S1). For PCR product identification we used 1 % agarose gel and an Axygen DNA purification kit (Suzhou, China) was used to purify PCR products. After purification, all PCR products were cloned into the sequencing vector pEASY-T3 (TransGen Biotech, China) and sequenced by Nanjing GenScript (Nanjing, China). Subsequently, a phylogenetic tree of HMGR was constructed and the three-dimensional structure of PtHMGR was determined according to the methods described by Zhang *et al.* (2017).

Vector construction and PtHMGR production

Depending on the analysis of restriction sites *PtHMGR* gene, BamHI and NotI were chosen as the restriction sites. Forward and reverse primers (Supplementary Data Table S1) were designed and the PCR procedure was performed as description above. Digestion with BamHI and NotI and ligation of *PtHMGR* yielded the recombinant vectors PET-28a-*PtHMGR* and PET-32a-*PtHMGR*, which were transformed into *Escherichia coli* BL21 (DE3), and PPICZα-A-*PtHMGR*, which was transformed into *Pichia pastoris* GS115.

Cells harbouring the PET-28a-*PtHMGR* and PET-32a-*PtHMGR* vectors were cultured in 100 mL of Luria–Bertani medium at 37 °C with shaking at 220 r.p.m. When the absorbance reached 0.6, 1.0 mM isopropyl-β-D-1-thiogalactopyranoside (IPTG) was added to induce production of PtHMGR. Following incubation for a further 4 h, the mixtures were resolved by 12 % SDS–PAGE.

Recombinant *P. pastoris* GS115 containing PPICZα-A-*PtHMGR* was cultured in 100 mL of buffered glycerol complex medium at 30 °C with shaking at 250 r.p.m. When the absorbance reached 2.0, we performed concentration at 5000 r.p.m. for 20 min at room temperature. The cells were resuspended in buffered methanol complex medium to an absorbance of ~1.0, transferred to a 1-L shake flask and incubated at 28 °C with shaking at 250 r.p.m. Methanol was added at 24-h intervals to a final concentration of 0.5–2 %. After centrifugation,

the supernatant was analysed by SDS–PAGE to determine the optimal culture duration and inducer concentration. Following centrifugation at 4 °C, PtHMGR was purified using a His-tag column and its identity was confirmed by western blotting with rabbit anti-His antibody as the first antibody and anti-rabbit IgG (TransGen Biotech) as the second antibody.

Assay of PtHMGR activity

PtHMGR activity was assayed using reaction mixtures containing 2.5 mmol K_2HPO_4 (pH 7.2), 5 mmol KCl, 1 mmol EDTA, 5 mmol DTT, 1 mg/mL PtHMGR and H_2O to 1 mL. The mixtures were heated in a water bath at 37 °C for 30 min and 30 mmol NADPH and 0.3 mmol HMG-CoA were added; the control lacked PtHMGR. The mixtures were incubated at 30 °C for 30 min and the reaction was terminated by the addition of 100 µL of 6 mol L^{-1} HCL. Finally, the mixture was passed through a 0.22-µm membrane and analysed using a Thermo TSQ 8000 EVO mass spectrometer.

High-performance liquid chromatography (HPLC; Shimadzu LC20A) conditions were as follows: solvents, 0.1 % formic acid, water and methanol; column temperature, 30 °C; flow rate, 0.3 mL min^{-1}; and a Waters XBridge C18 3.5 µm, 2.1 × 150 mm column. The mass spectrometer (Thermo TSQ 8000 EVO) conditions were as follows: SCIEX triple TOF 5600+ *m*/*z* range, 50–1200; ion collection, IDA pattern; and second level, CE 35, CES 20 and an information-dependent acquisition (IDA) pattern to collect ions.

Quantitative reverse transcriptase–polymerase chain reaction

In order to analyse *PtHMG*R expression level in various tissues, we extracted RNA from mature and young leaves, upper and lower stems, petioles and roots (Supplementary Data Fig. S1). In addition, RNA was extracted from *P. trichocarpa* leaves treated different stress conditions and then reverse-transcribed to form cDNA. A pair of specific primers (Supplementary Data Table S1) and SYBR Green Master Mix (Roche) were used for quantitative reverse transcription–polymerase chain reaction (qRT–PCR) amplification of *PtHMG*R. Three independent biological experiments were performed. *Ptactin* (accession number XM-006370951.1) was used as the internal reference. Fold changes in expression levels were calculated by the $^{\Delta\Delta}$CT method (fold change = 2−[$^{\Delta\Delta}$CT]) (Livak and Schmittgen, 2001). Real-time RT–PCR reactions were performed using SYBR Green Mix (Roche) under the following conditions: initial incubation at 95 °C for 5 min followed by 40 cycles of 30 s at 95 °C and 30 s at the annealing temperature of 60 °C. Three independent biological experiments were performed.

Transformation of Populus × euramericana 'Nanlin895' and screening of transgenic lines

The ORF of *PtHMGR* was inserted into the vector pENTR/D-TOPO and subsequently into the destination vector pGWB9. The recombinant vector pGWB9-*PtHMGR* was transformed into *Agrobacterium* EHA105 and transgenic poplar lines were generated by the method of leaf infecting (Zhang *et al.*, 2017).

The seedlings were cultured in screening differentiation medium (MS medium supplemented with 30 mg mL^{-1} kanamycin, 200 mg mL^{-1} cefotaxime, 30 g L^{-1} sucrose, 8 g L^{-1} agar, 0.5 mg L^{-1} *N*-6-benzyladenine and 0.002 mg L^{-1} thidiazuron at pH 5.8) and screening bud elongation medium (MS medium supplemented with 20 mg mL^{-1} kanamycin, 200 mg mL^{-1} cefotaxime, 30 g L^{-1} sucrose, 8 g L^{-1} agar, 0.5 mg L^{-1} *N*-6-benzyladenine and 0.002 mg L^{-1} thidiazuron at pH 5.8) and subsequently transferred to screening rooting medium (half-strength MS medium supplemented with 10 mg mL^{-1} kanamycin, 200 mg mL^{-1} cefotaxime, 30 g L^{-1} sucrose and 8 g L^{-1} agar at pH 5.8). Genomic DNA and RNA were isolated from the leaves of ten putative transgenic lines and subjected to PCR to verify whether *PtHMGR* was present in poplar chromosomes and could be expressed. The PCR reaction was carried out under the following conditions: 95 °C for 10 min; 35 cycles of 95 °C for 2 min, 58 °C for 2 min and 72 °C for 2 min; and 72 °C for 10 min. PCR products were visualized on a 1 % agarose gel. Subsequently, real-time qRT–PCR was carried out to reveal the transcript levels of *PtHMGR* in the transformants and WT poplars. The reaction conditions and reaction system for real-time qRT–PCR used for the transformants and WT poplars were as described above. Three independent biological experiments were performed.

Phenotypic analysis of transgenic poplar

Two-month-old T_1 seedlings were transferred to half-strength MS medium without (control) or with 50, 100 or 150 mM NaCl or 1, 2 or 3 % PEG_{6000} for 1 month. Next, root length was evaluated (three plants of each line were used for each NaCl concentration and PEG_{6000} concentration). Following treatment for 20 d with 100 mM NaCl and 2 % PEG_{6000}, leaves were subjected to RNA extraction for analysis of transcript levels of indole-3-acetaldehyde oxidase (*AAO3*), ABA-insensitive 1 (*ABI1*), cold-regulated 15A (*COR15A*), *KIN*, *MYB*, *MYC2* and responsive to dehydration 22 (*RD22*) (the forward and reverse primers are shown in Supplementary Data Table S1). The reaction conditions and reaction system for real-time qRT–PCR used for the transformants and WT poplars were as described above. Three independent biological experiments were performed.

Transplantation of WT and transgenic poplar and assay of salt- and drought-stress tolerance

Two-month-old WT and transgenic poplars cultured in a greenhouse were transplanted to pots containing soil mixed with sterilized peat and perlite (2:1) and grown under long-day conditions (16 h light/8 h dark) at 24 °C for 5 months. Next, the plants were irrigated for 2 weeks with a solution containing 200 mM NaCl. Drought stress was induced by withdrawing irrigation for 2 weeks. The poplars were grown under long-day (16 h light/8 h dark) conditions.

The leaves were collected and RNA was extracted and subjected to qRT–PCR analysis of the transcript levels of ascorbate peroxidase (*APX*), catalase (*CAT*), glutathione *S*-transferase

(*GST*), superoxide dismutase (*SOD*), respiratory burst oxidase homologue protein A (*RbohA*) and *RbohB* (the forward and reverse primers are shown in Supplementary Data Table S1). In addition, the effects of drought and salt stress on the proline and malondialdehyde (MDA) levels and the activities of SOD and peroxidase (POD) were evaluated using a microplate reader (Bio-Rad).

ABA-mediated signal transduction

Drought, salt and low and high temperatures increase the accumulation of ABA, an important hormone in plant responses to abiotic stresses. Indeed, the ABA signalling pathway is pivotal in plant responses to drought and high salt levels (Zhu, 2000). Higher plants synthesize ABA by direct and indirect pathways. In the direct pathway, mevalonate is converted to ABA in a manner dependent on pyrophosphate. In the indirect pathway, ABA is generated by oxidative cleavage of a carotenoid precursor; this is the major ABA synthesis pathway Seo and Koshiba, (2002). The rate-limiting enzymes in ABA synthesis are NCED and zeaxanthin (Zhang *et al.*, 2009; Sun *et al.*, 2012; Jing *et al.*, 2018). We evaluated the expression levels of genes related to the mevalonate and MEP pathways and ABA synthesis-related genes (forward and reverse primers are shown in Supplementary Data Table S1) in WT and transgenic poplars. The reaction conditions and reaction system for real-time qRT–PCR used for the transformants and WT poplars were as described above. Three independent biological experiments were performed.

RESULTS

Molecular cloning and sequence analysis of PtHMGR

The ORF of *PtHMGR* (XP_002317026.1) was 1767 bp and encoded 588 amino acids (Supplementary Data Fig. S2). The molecular weight of PtHMGR was 62.7 kDa and its isoelectric point was 6.24. PtHMGR contained multiple active domains at the C-terminus: two HMG-CoA-binding domains, EMPVGYIQIP and TTEGCLVA; and two NADP(H)-binding domains, DAMGMNMV and VGTVGGGT (Supplementary Data Fig. S3). The conserved domains were consistent with the reported structural characteristics of plant HMGR proteins. In addition, the C-terminal amino acid sequences were highly conserved, while those at the N-terminus were not (Supplementary Data Fig. S3).

Three-dimensional structure and phylogenetic tree of PtHMGR

The three-dimensional structures of the HMGRs of *P. trichocarpa*, *Arabidopsis thaliana*, *Nicotiana tabacum*, *Oryza sativa* and *Zea mays* were determined. The HMG-CoA- and NADPH-binding domains were conserved, and their spatial structures were similar (Supplementary Data Fig. S4). PtHMGR showed 73.27, 64.63, 62.96 and 41.03 % similarity with the HMGRs of *N. tabacum*, *O. sativa*, *A. thaliana* and *Z. mays,* respectively (Supplementary Data Fig. S4).

In the phylogenetic tree of PtHMGR and 37 other HMGRs, PtHMGR was clustered with *Jatropha curcas* and *Cephalotus follicularis* (Fig. 1). Because plant *HMGR*s are relatively conserved, this will be useful for studies of genetic differentiation and molecular evolution.

Expression and purification of PtHMGR

Following cloning of the ORF of *PtHMGR* into PET-28a (Figure 2A) and IPTG-induced expression in *E. coli* BL21 (DE3), the target protein was not detected by 12 % SDS–PAGE (Fig. 2B). The ORF of *PtHMGR* was also cloned into PET-32a (Fig. 2C), but the Trx-tagged target protein was not detected by 12 % SDS–PAGE (Fig. 2D).

The ORF of *PtHMGR* was cloned into pPICZα (Fig. 2E) and the recombinant plasmid pPICZα-A-*PtHMGR* was transformed into *P. pastoris* GS115 by electroporation. The greatest yield of the target protein resulted from the addition of 1 % methanol for 72 h (Fig. 2F, G). The His-tagged recombinant protein was purified using Ni-IDA resin and its identity was confirmed by western blotting (Fig. 2H).

Functional analysis of PtHMGR

HMGR catalyses the reaction of one molecule of HMG-CoA with two molecules of reduced NADPH. First, one molecule of NADPH is desorbed from H and added to the acyl oxygen bound to CoA in HMG-CoA. Next, the CoA molecule is detached from HMG to form the intermediate mevalonaldehyde and CoASH, and finally the H of the other NADPH molecule is added to the acid oxygen of mevalonaldehyde to produce mevalonate (Ha *et al.*, 2001; Yechun *et al.*, 2007).

We evaluated the activity of HMGR *in vitro*. Mevalonate was produced by the reactions containing PtHMGR (Fig. 4), but not by the control reactions (Fig. 3). Therefore, PtHMGR catalyses the formation of mevalonate by HMG-COA. The Michaelis constant of PtHMGR for HMG-CoA was 7.91 ± 3.04 (Supplementary Data Fig. S5).

PtHMGR *transcript levels*

In this study, *PtHMGR* expression was higher in roots, followed by mature leaves, stems, young leaves and petioles (Fig. 5A). The root is the vegetative organ and is responsible for absorbing water from soil as well as dissolving inorganic salts therein, provides structural support, and stores organic substances. Therefore, we speculated that *PtHMGR* may be related to the growth, development and response to plant osmotic stress.

We determined the effect on *PtHMGR* expression of ABA, JA, SA, NaCl, PEG_{6000}, H_2O_2 and cold stress. Treatment with 200 μM ABA resulted in a gradual increase in *PtHMGR* expression to a peak at 6 h followed by a decrease to a higher level than the control (Fig. 5B). The increase in *PtHMGR* expression to a peak at 12 h and a subsequent decrease caused by 200 μM JA was of lesser magnitude than that caused by

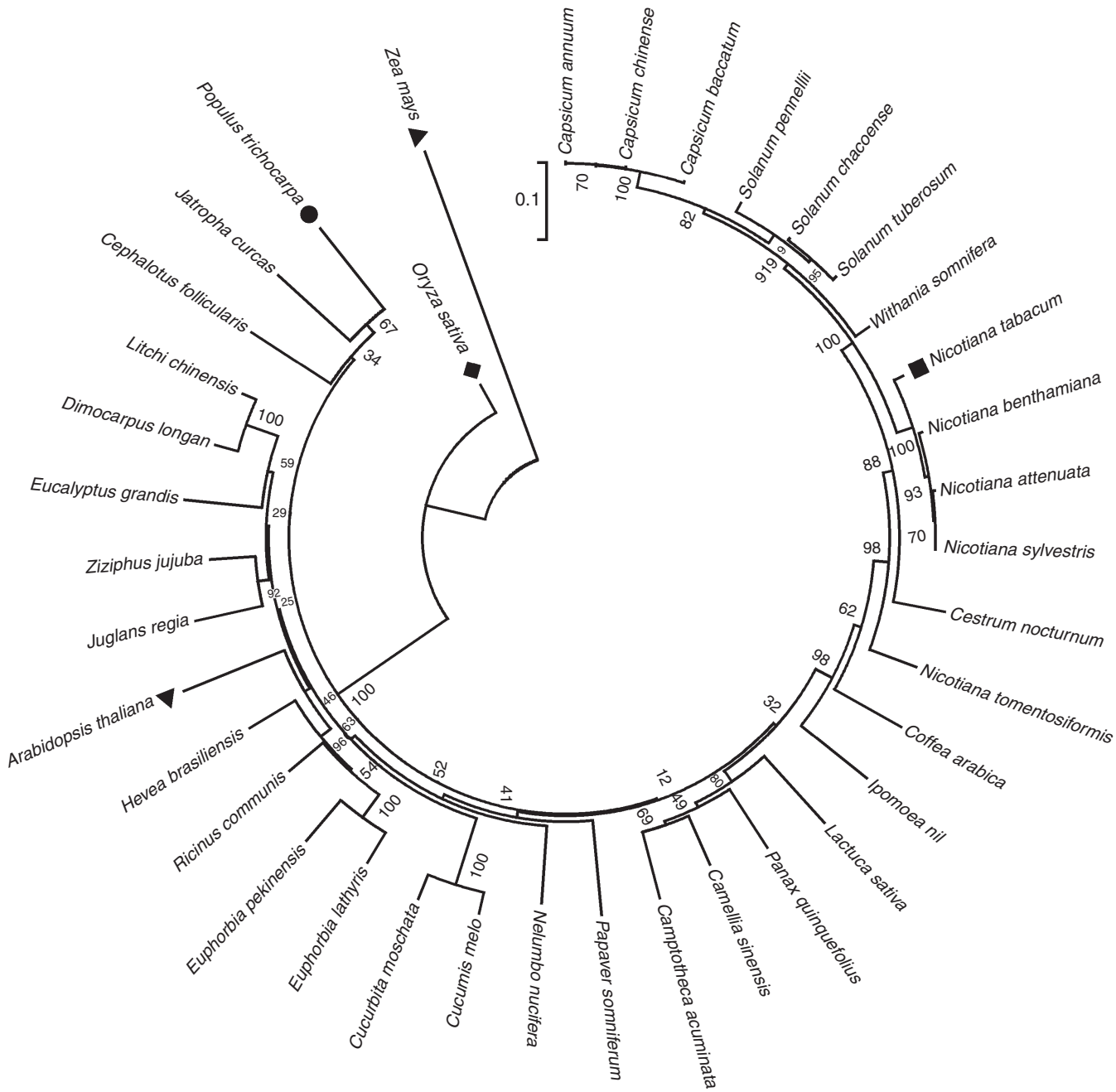

FIG. 1. Phylogenetic tree of PtHMGR and other HMGRs. The GenBank accession numbers of the HMGRs are as follows: *Populus trichocarpa*, XM_002316990.2; *Arabidopsis thaliana*, NM_106299.4; *Camellia sinensis*, KF649853.1; *Camptotheca acuminata*, AAB69727.1; *Capsicum annuum*, XM_016704840.1; *Capsicum baccatum*, MLFT02000002.1; *Capsicum chinense*, CIT02000002.1; *Cephalotus follicularis*, BDDD01003560.1; *Cestrum nocturnum*, KY703396.1; *Coffea arabica*, HQ540670.1; *Cucumis melo*, NM_001297451.1; *Cucurbita moschata*, XM_023090472.1; *Dimocarpus longan*, JN034591.1; *Eucalyptus grandis*, XM_010062927.2; *Euphorbia lathyris*, JQ694150.1; *Euphorbia pekinensis*, EF062569.1; *Hevea brasiliensis*, XM_021830837.1; *Ipomoea nil*, XM_019327336.1; *Jatropha curcas*, XM_012232190.2; *Juglans regia*, XM_018987497.1; *Lactuca sativa*, XM_023892538.1; *Litchi chinensis*, JN034589.1; 728.1; *Nicotiana benthamiana*, LC382275.1; *Nicotiana sylvestris*, XM_009782484.1; *Nicotiana tabacum*, NM_001326284.1; *Nicotiana tomentosiformis*, XM_009602774.2; *Oryza sativa*, AF110382.1; *Panax quinquefolius*, FJ755158.2; *Papaver somniferum*, XM_026548454.1; *Ricinus communis*, XM_002510686.3; *Solanum chacoense*, JF802615.1; *Solanum pennellii*, XM_015210528.1; *Solanum tuberosum*, NM_001288155.1; *Withania somnifera*, KX574809.1; *Zea mays*, NM_001153261.1; and *Ziziphus jujuba*, XM_016024520.2. The tree was constructed using the neighbor-joining method in MEGA 5.1 and bootstrapped 1000 times. Bootstrap percentages are indicated at the branch points. In all cases, tree topologies obtained using the NJ, minimum evolution, and maximum parsimony methods were identical. The numbers on the nodes represent the bootstrap values.

200 μM ABA (Fig. 5C). Treatment with JA resulted in significant upregulation of *PtHMGR* expression to a peak at 3 h (Fig. 5D). Treatment with 200 mM NaCl resulted in an increase in the expression of *PtHMGR* to a peak at 12 h, followed by a gradual

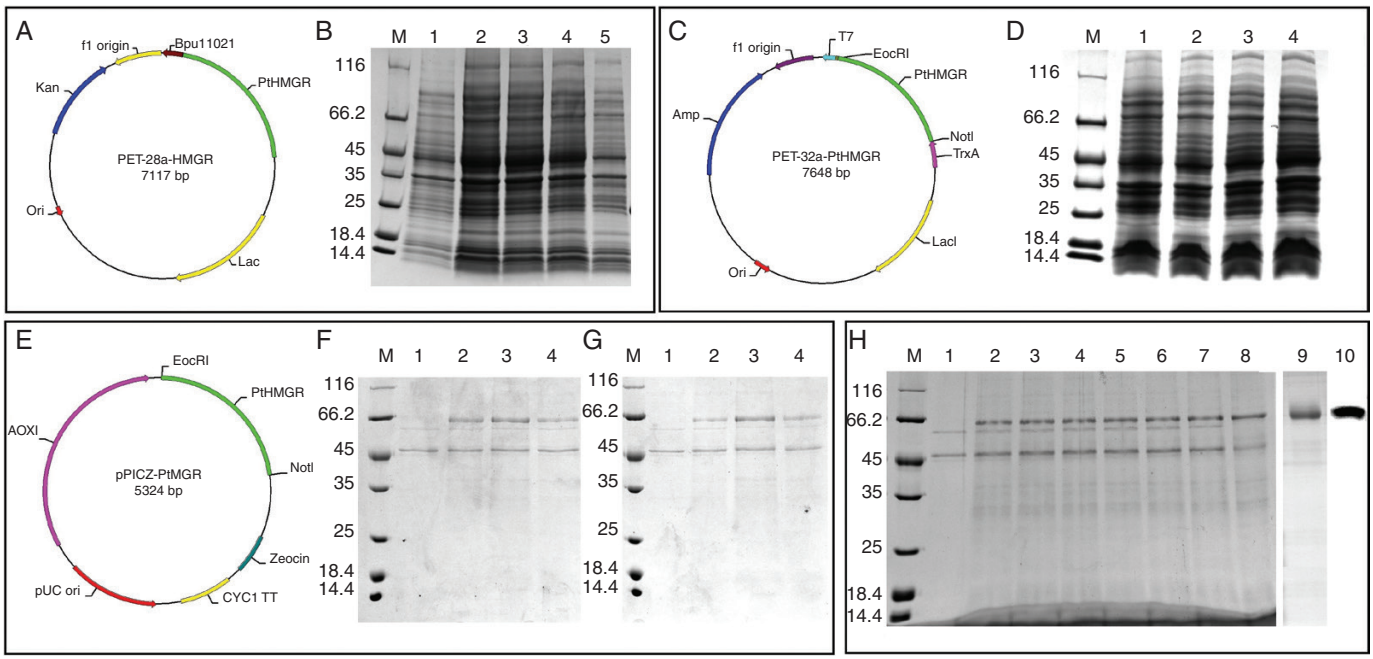

FIG. 2. PtHMGR protein production and purification. (A) Construction of the PET-28a fusion vector containing *PtHMGR* and BamHI and NotI sites. (B) Analysis of PET-28a-HMGR expression by 12 % SDS–PAGE. Lane M, molecular mass marker; lane 1, negative control; lanes 2–5, colonies 1–4, respectively, induced by 1 mM IPTG. (C) Construction of the PET-32a fusion vector containing *PtHMGR* and BamHI and NotI sites. (D) Analysis of PET-28a-HMGR expression by 12 % SDS–PAGE. Lane M, molecular mass marker; lane 1, negative control; lanes 2–4, colonies 1–3, respectively, induced by 1 mM IPTG. (E) Construction of the pPICZ-α fusion vector containing *PtHMGR* and BamHI and NotI sites. (F) Analysis of methanol-induced pPICZ-α-HMGR expression. Lane M, molecular mass marker; lane 1, negative control; lane 2, 0.5 % methanol for 48 h; lane 3, 1 % methanol for 48 h; lane 4, 2 % methanol for 48 h. (G) Analysis of methanol-induced pPICZ-α-HMGR expression. Lane M, molecular mass marker; lane 1, negative control; lane 2, 1 % methanol for 48 h; lane 3, 1 % methanol for 72 h; lane 4, 1 % methanol for 96 h. (H) Analysis of the expressed fusion protein by 12 % SDS–PAGE. Lane M, molecular mass marker; lane 1, negative control; lanes 2–8, colonies 1–7, respectively, induced by 1 % methanol for 72 h; lane 9, purified PtHMGR; lane 10, identification of PtHMGR by western blotting.

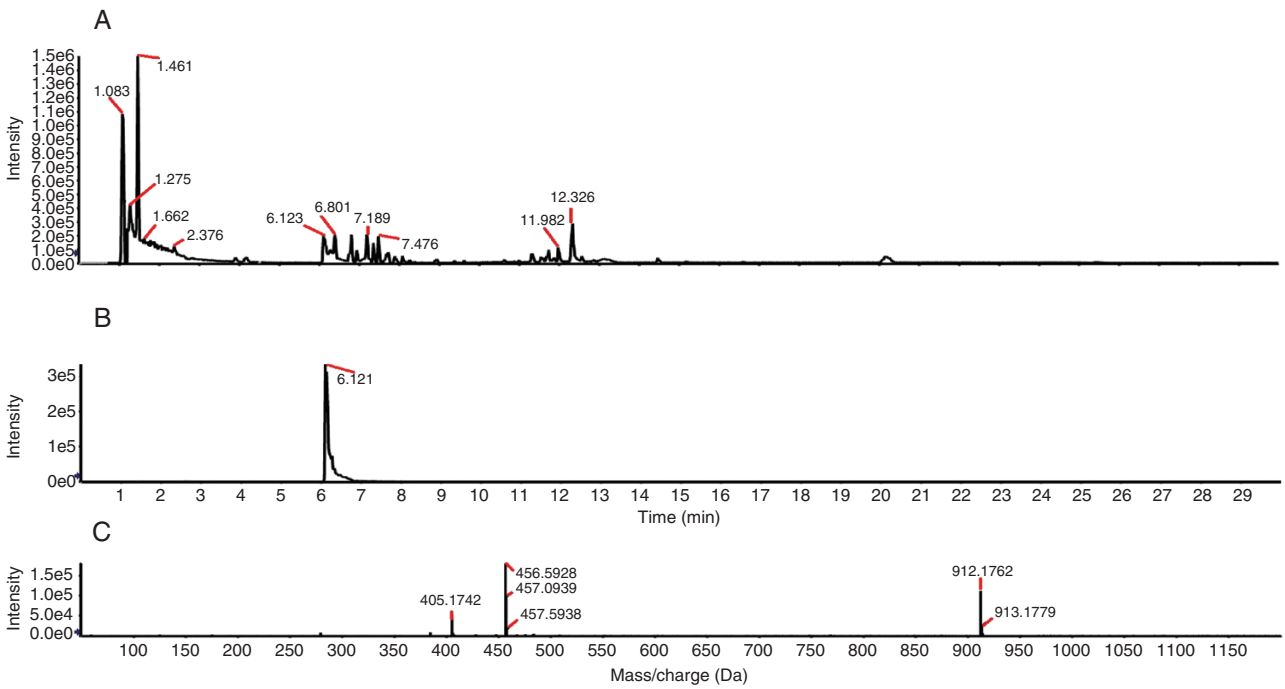

FIG. 3. Activity of the control *in vitro*. (A) Total ion chromatogram of the reaction products; (B) XIC peak map; (C) TOF–MS peak map.

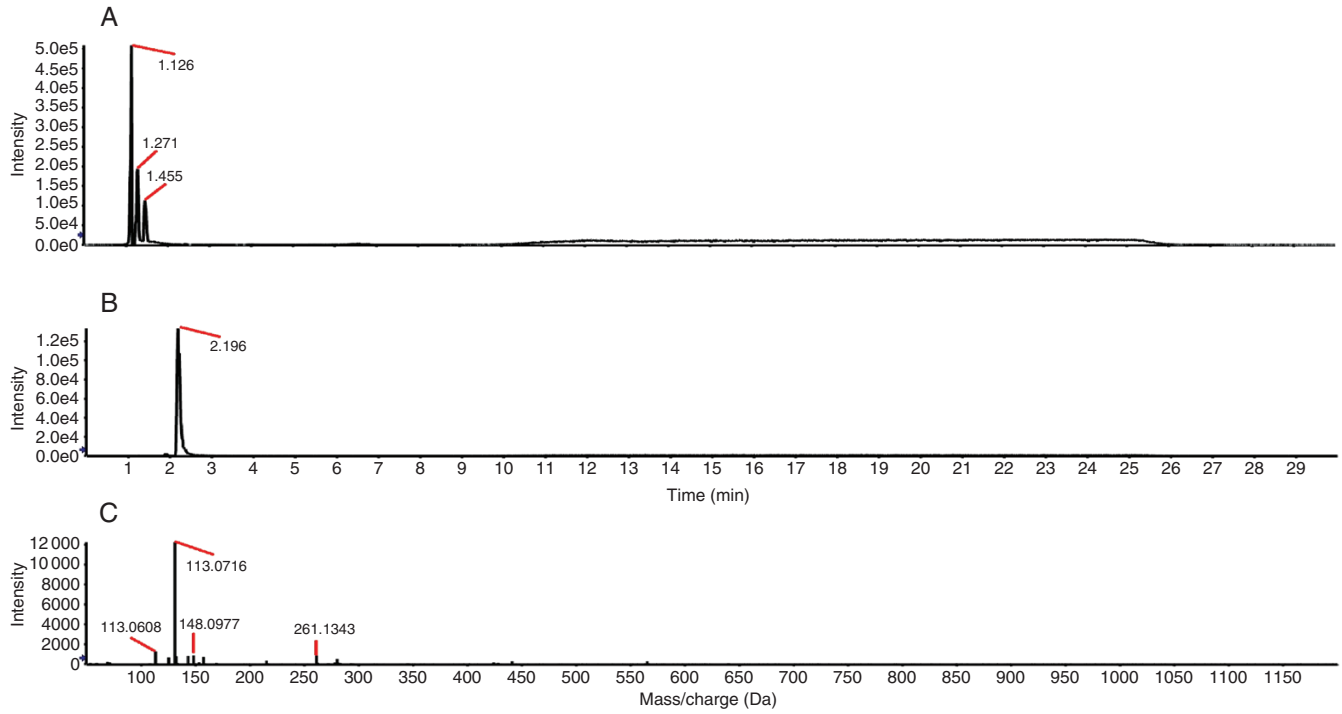

FIG. 4. Activity of PtHMGR *in vitro*. (A) Total ion chromatogram of the reaction products; (B) XIC peak map; (C) TOF–MS peak map.

decrease from 24 to 48 h (Fig. 5E). Treatment with 2 mM H_2O_2 resulted in an increase in *PtHMGR* expression from 1 to 3 h, followed by a slight decrease at 6 h and a subsequent increase to a peak at 48 h (Fig. 5F). Treatment with 10 % PEG_{6000} increased *PtHMGR* expression at 1 to 48 h with a peak at 24 h; at 6 h, *PtHMGR* expression was ~16-fold higher than the control (Fig. 5G). Therefore, the expression of *PtHMGR* is modulated by a variety of stresses, indicating an important role in plant resistance to drought and salt stress.

Identification of transgenic poplar plants and analysis of stress resistance

Successful generation of ten transgenic poplar lines was confirmed by RT–PCR (Supplementary Data Fig. S6A). *PtHMGR* expression was higher in transgenic lines than in WT (Supplementary Data Fig. S6B). Therefore, *PtHMGR* was successfully introduced into the *Populus* × *euramericana* 'Nanlin895' genome. Growth of transgenic poplars was slower in half-strength MS medium containing 150 mM NaCl than in half-strength MS medium alone, while WT growth was inhibited in half-strength MS medium containing 100 or 150 mM NaCl (Fig. 6A). The roots of transgenic poplars were longer than those of WT under normal growth conditions. Salt stress induced significant differences in the lengths of roots of transgenic and WT poplars (Fig. 6B). The transgenic poplars grew in medium containing 3 % PEG_{6000}, while WT growth was significantly inhibited by 2 % PEG_{6000} (Fig. 6A). In addition, the roots of transgenic poplars grown in 1–3 % PEG_{6000} were longer than those of WT poplars (Fig. 6C). Therefore, the transgenic poplars were better adapted to osmotic stress than were the WT poplars.

PtHMGR regulates the expression of stress-related genes

We assessed the effect of drought and salt stress on the transcript levels of *AAO3*, *ABI*, *COR15A*, *KIN*, *MYB*, *MYC* and *RD22* in transgenic and WT poplars. Under normal growth conditions, the transcript levels of these genes differed significantly between transgenic and WT poplars. The transcript level of *AAO3* in transgenic lines was higher than that in WT under normal conditions but was lower in transgenic lines under salt treatment (Fig. 7A). The transcript level of *ABI* showed similar trends to that of *AAO3* (Fig. 7B). In addition, the transcript levels of *COR15A* and *KIN* in transgenic and WT poplars were increased by salt treatment. It was more obvious that the expression of *COR15A* and *KIN* in transgenic lines was increased by salt treatment (Fig. 7C, D). The transcript level of *MYB* in transgenic and WT poplars was upregulated by salt treatment (Fig. 7E). The transcript level of *MYC2* in transgenic and WT poplars was increased by salt treatment and was higher in the latter irrespective of salt treatment (Fig. 7F). The transcript level of *RD22* in transgenic lines was higher than that in WT but was decreased by salt treatment; the magnitude of the decrease was greater in transgenic lines (Fig. 7G).

Under normal growth conditions, the transcript levels of *AAO3* and *KIN* in transgenic lines were higher than those in WT.

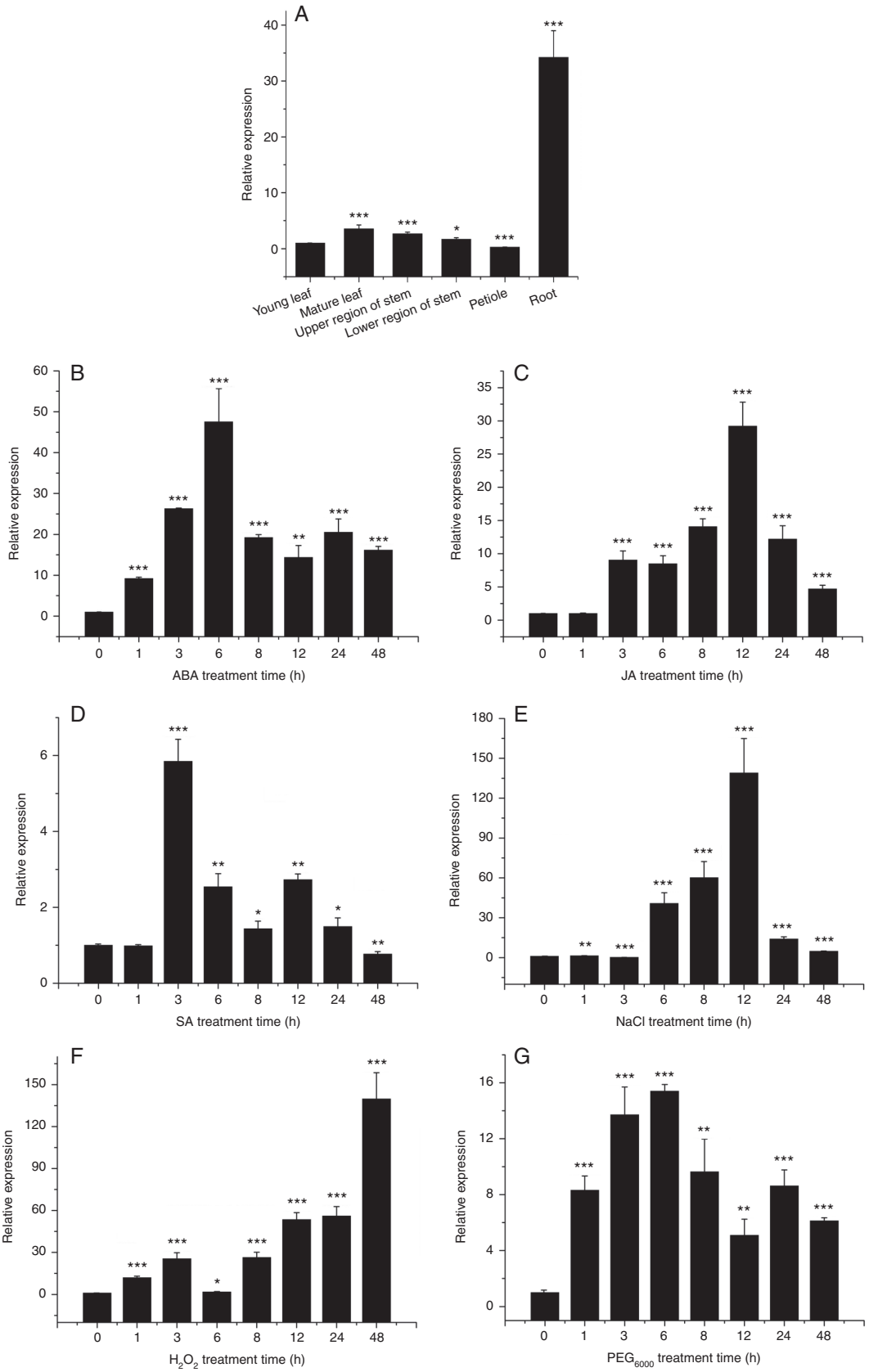

FIG. 5. (A) Transcript levels of *PtHMGR* gene of *P. trichocarpa* in mature leaves, young leaves, upper and lower region of stems, roots and petioles. Effect of (B) 200 μM ABA, (C) 200 μM JA, (D) 200 μM SA, (E) 200 mM NaCl, (F) 2 mM H_2O_2, and (G) 10 % PEG_{6000} on the *PtHMGR* transcript level. Relative expression was calculated using *Actin* as an internal reference. Leaves treated with distilled water served as controls. Vertical bars are mean ± s.d. ($n = 3$). Three independent experiments were performed. *$P < 0.05$, **$P < 0.01$, ***$P < 0.001$.

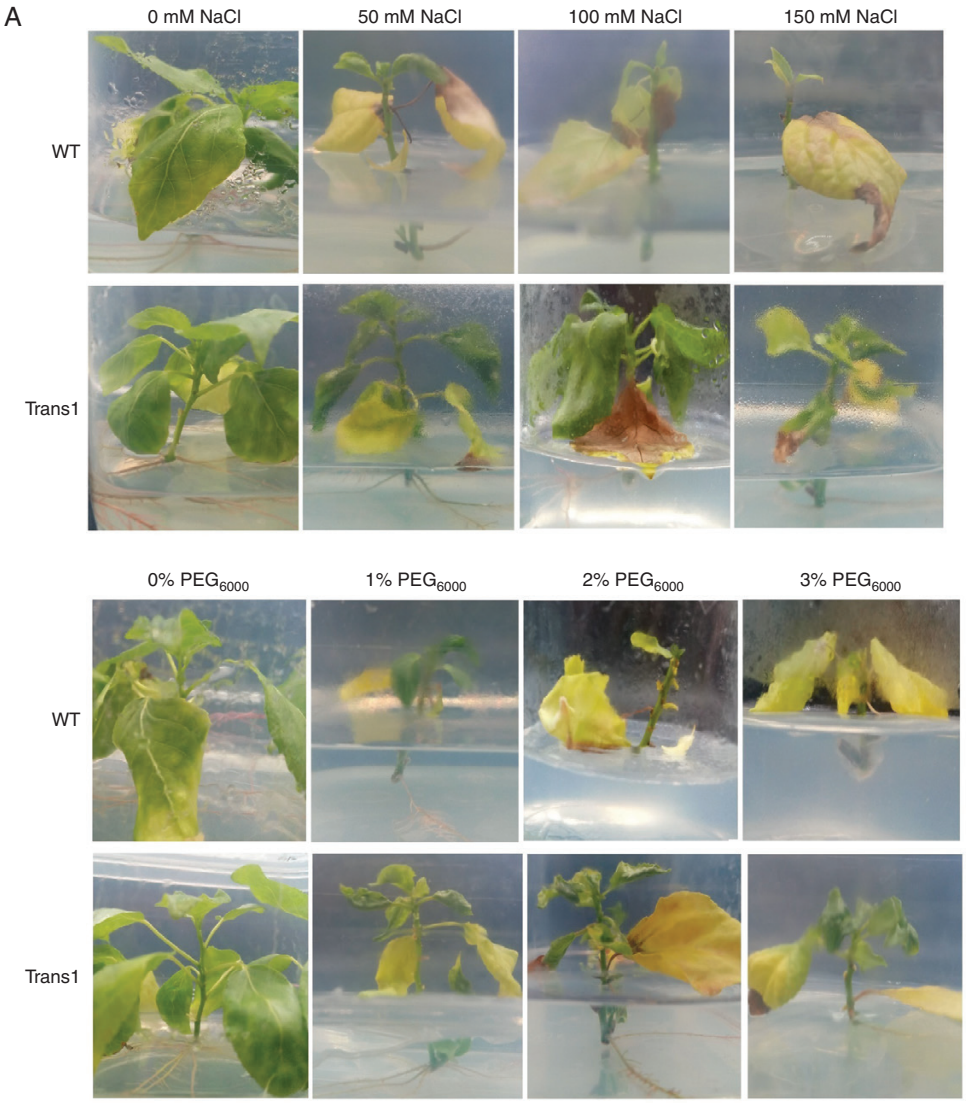

Fig. 6. (A) Phenotype of WT and transgenic poplars treated with 0, 50 or 100 mM NaCl or 1, 2 or 3 % PEG_{6000} in WT and transgenic poplar. (B) Root length in MS medium containing 0, 50 or 100 mM NaCl or (C) 1, 2 or 3 % PEG_{6000}. Three independent experiments were performed. *$P < 0.05$, **$P < 0.01$, ***$P < 0.001$.

Treatment with PEG_{6000} resulted in upregulation of *AAO3*, *KIN*, *ABI* and *COR15A* expression (Fig. 8A–D). Under PEG_{6000} treatment, the transcript levels of *ABI* and *COR15A* in transgenic lines were lower than those in WT (Fig. 8B and C). There was no difference in *MYB* expression between the transgenic and WT poplars, but *MYB* expression was increased by PEG_{6000} treatment (Fig. 8E). Under PEG_{6000} treatment, the transcript level of *MYC2* was increased, and the increase in WT was significant. The decrease in the transcript level of *RD22* induced by PEG_{6000} treatment was greater in WT than in transgenic lines. Therefore, *PtHMGR* responds to environmental stress by altering the expression of stress-related genes.

Overexpression of PtHMGR improves drought tolerance

Overproduction of ROS can cause oxidative damage to plant cells (Xiuli *et al.*, 2006; Choudhury *et al.*, 2017). To determine whether *PtHMGR* modulates ROS accumulation, we analysed the expression of genes related to antioxidants (*SOD*, *CAT*, *GST* and *APX*) and ROS generation (*RbohA* and *RbohB*) by qRT–PCR. Growth of WT was significantly inhibited by drought stress, and the leaves turned yellow and fell off. Some leaves of transgenic lines also fell off (Fig. 9A). The transcript levels of *APX*, *CAT*, *GST* and *SOD* were increased significantly under the drought condition, and expression of *APX*, *CAT*, *GST* and *SOD* in transgenic lines showed greater increases than in WT (Fig. 9B–E). *RbohA* expression was significantly higher in WT than in transgenic lines and was increased by drought stress (Fig. 9F). Moreover, although the expression of *RbohB* was increased under drought stress, it was lower in transgenic lines than in WT (Fig. 9G).

We also analysed the activities of POD, SOD and CAT, and MDA and proline contents. The MDA level in transgenic lines was slightly lower than that in WT under normal conditions

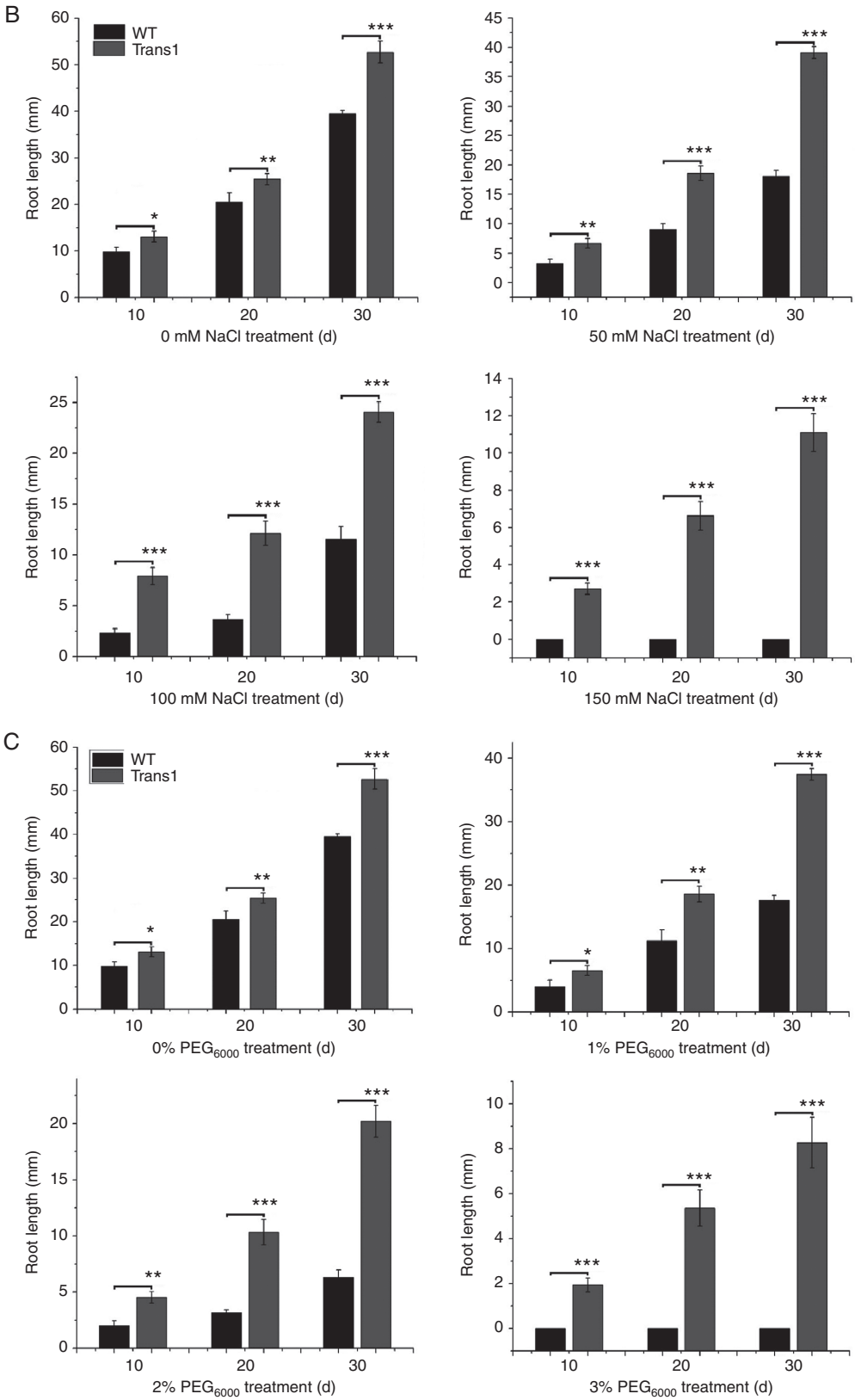

FIG. 6. Continued

(Fig. 10A). In addition it increased, the MDA level in WT was higher than that in transgenic lines under drought stress. The activities of SOD, POD and CAT and proline content were higher in transgenic lines compared with WT under drought stress (Fig. 10B–E). These results suggest that *PtHMGR* modulates the expression of genes related to ROS scavenging, the activities of SOD, POD and CAT, and the MDA and proline contents of plant cells.

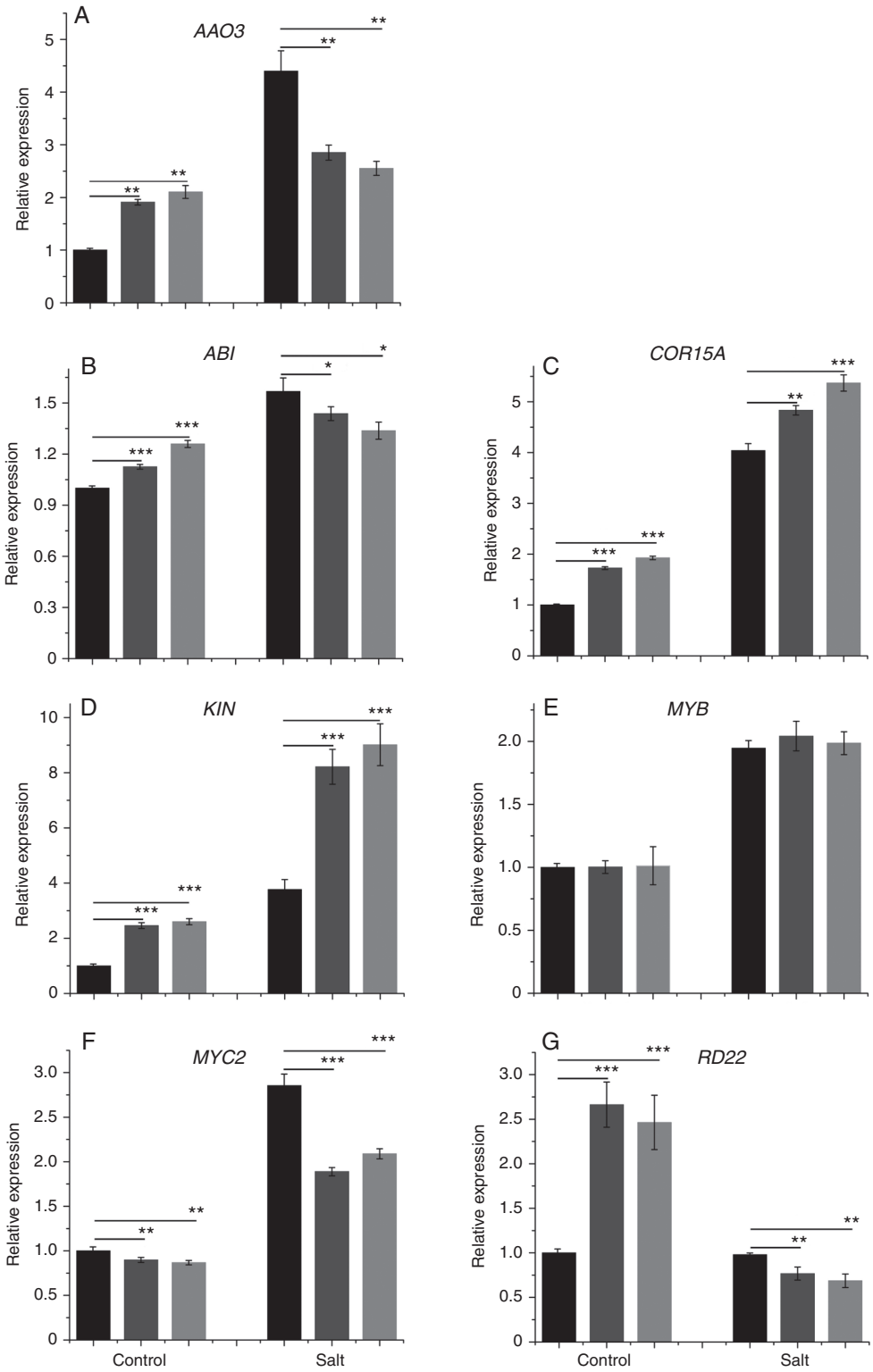

FIG. 7. Effect of treatment with 100 mM NaCl on the transcript level of (A) *AAO3*, (B) *ABI*, (C) *COR15A*, (D) *KIN*, (E) *MYB*, (F) *MYC2* and (0G) *RD22*. Relative expression was calculated using *Actin* as an internal reference. WT leaves untreated with NaCl served as controls. Vertical bars are mean ± s.d. ($n = 3$). Black columns, WT; Trans1 and Trans2 represent two relatively independent transgenic lines, respectively, dark grey columns, Trans1; light grey columns, Trans2. Three independent experiments were performed. *$P < 0.05$, **$P < 0.01$, ***$P < 0.001$.

Overexpression of PtHMGR improves salt tolerance

Osmotic stress leads to osmotic imbalance and physiological disorders, thus inhibiting the growth and development of plants (Ahuja *et al.*, 2010). Growth of WT was significantly inhibited by salt stress, and leaves turned yellow and fell off. Some leaves of the transgenic lines also fell off (Fig. 11A). The transcript levels of *APX*, *CAT*, *GST* and *SOD* were increased significantly

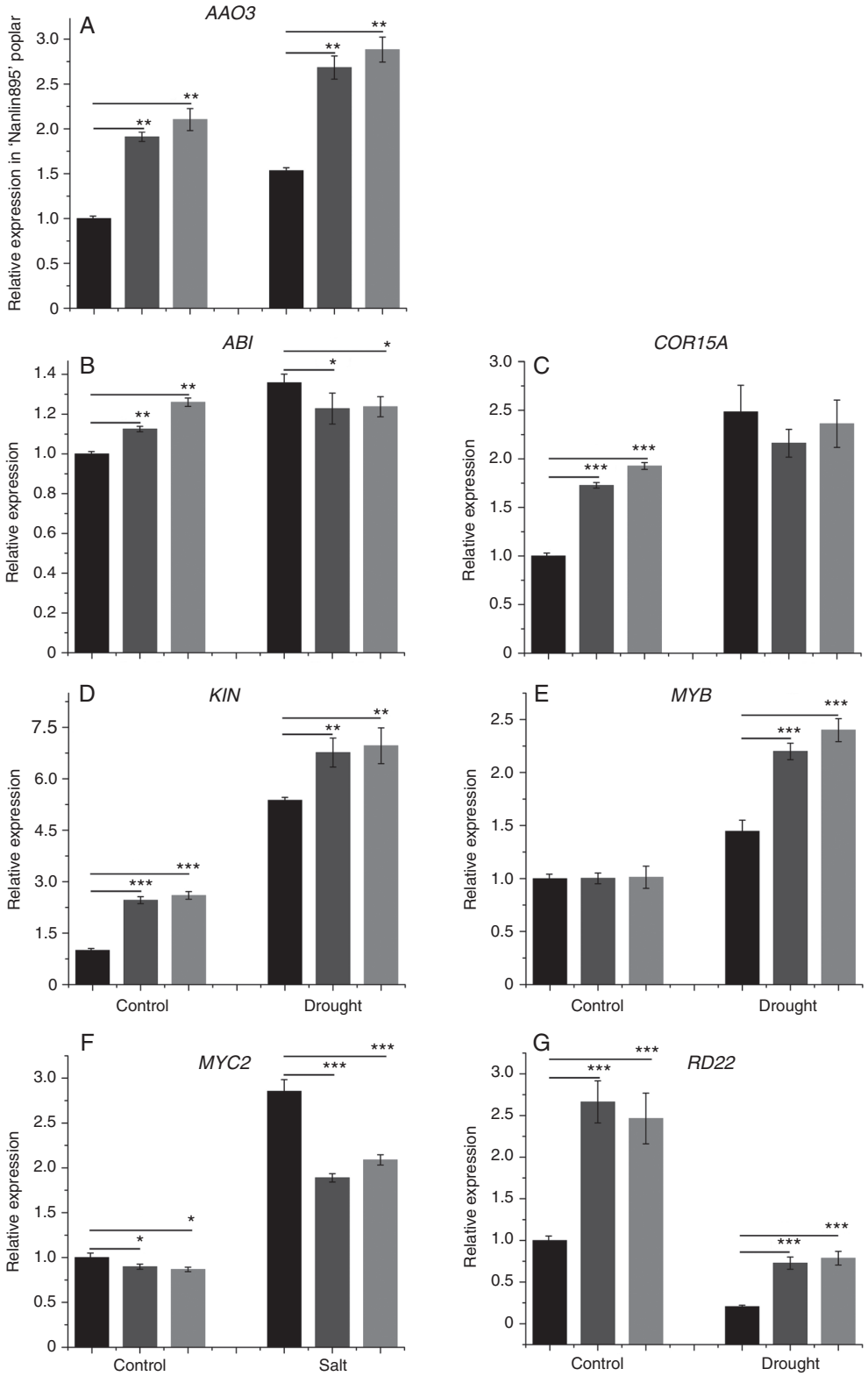

FIG. 8. Effect of treatment with 2 % PEG_{6000} on the transcript level of (A) *AAO3*, (B) *ABI*, (C) *COR15A*, (D) *KIN*, (E) *MYB*, (F) *MYC2* and (G) *RD22* in WT and transgenic poplar. Relative expression was calculated using *Actin* as an internal reference. WT leaves untreated with PEG_{6000} served as controls. Vertical bars are mean ± s.d. ($n = 3$). Black columns, WT; Trans1 and Trans2 represent two relatively independent transgenic lines, respectively, dark grey columns, Trans1; light grey columns, Trans2. Three independent experiments were performed. *$P < 0.05$, **$P < 0.01$, ***$P < 0.001$.

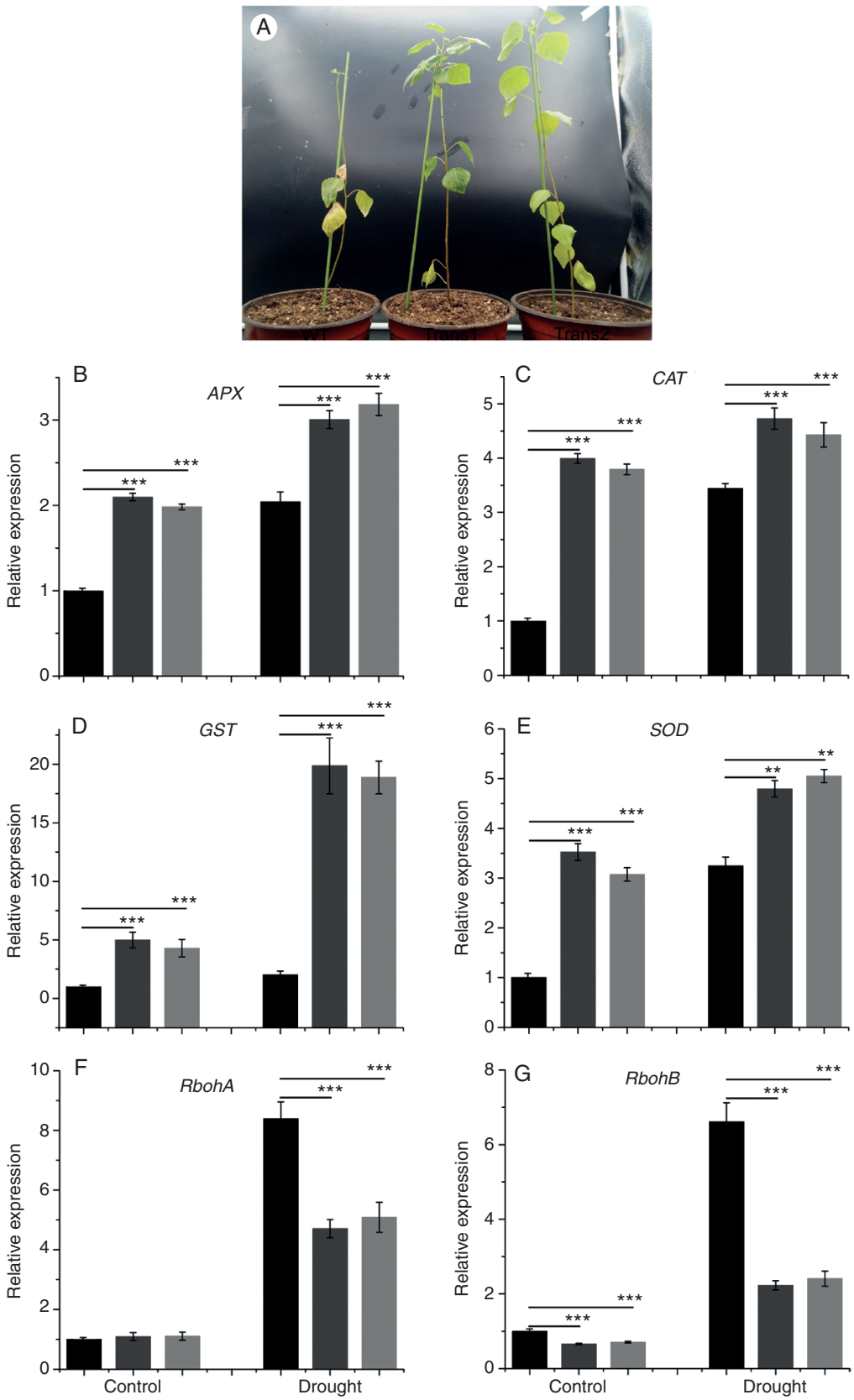

FIG. 9. Effect of drought stress on the (A) phenotype and transcript levels of (B) *APX*, (C) *CAT*, (D) *GST*, (E) *SOD*, (F) *RbohA* and (G) *RbohB* in WT and transgenic poplar. Relative expression was calculated using *Actin* as an internal reference. WT leaves untreated with drought stress served as controls. Vertical bars are mean ± s.d. ($n = 3$). Black columns, WT; Trans1 and Trans2 represent two relatively independent transgenic lines, respectively, dark grey columns, Trans1; light grey columns, Trans2. Three independent experiments were performed. $^{**}P < 0.01$, $^{***}P < 0.001$.

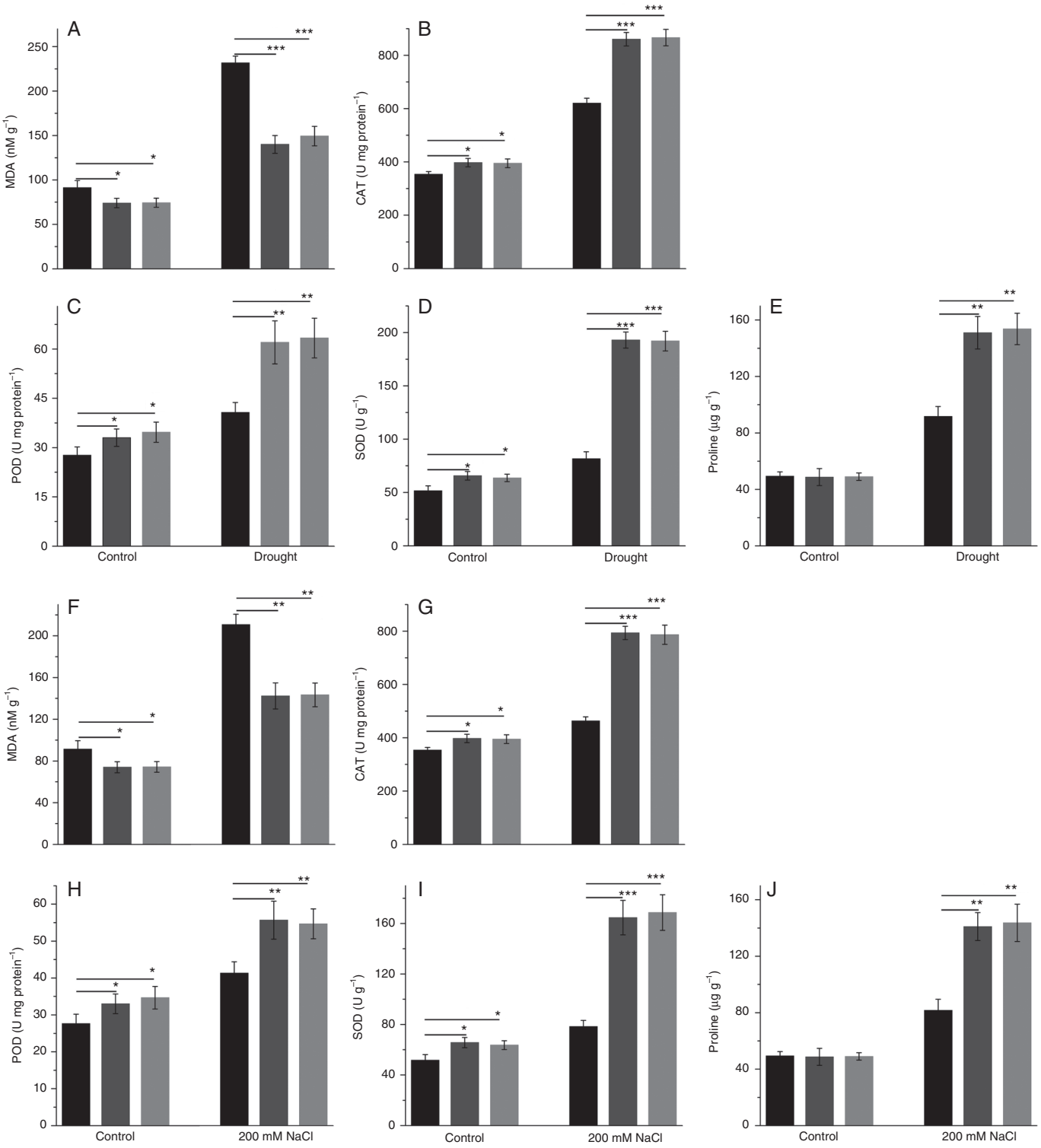

FIG. 10. (A–E) Effect of drought stress on (A) MDA level, (B) CAT activity, (C) POD activity, (D) SOD activity and (E) proline content in WT and transgenic poplar. (E–J) Effect of salt stress on (F) MDA level, (G) CAT activity, (H) POD activity, (I) SOD activity and (J) proline content in WT and transgenic poplar. Vertical bars are mean ± s.d. ($n = 3$). Black columns, WT; Trans1 and Trans2 represent two relatively independent transgenic lines, respectively, dark grey columns, Trans1; light grey columns, Trans2. Three independent experiments were performed. *$P < 0.05$, **$P < 0.01$, ***$P < 0.001$.

and the increases in the transcript levels of *APX*, *CAT*, *GST*, and *SOD* in transgenic lines were greater than those in WT under salt stress (Fig. 11B–E). Although the expression of *RbohA* was increased by salt stress, the transcript level of *RbohA* in transgenic lines was significantly lower than that in WT (Fig. 11F). The expression of *RbohB* in transgenic lines was lower than that

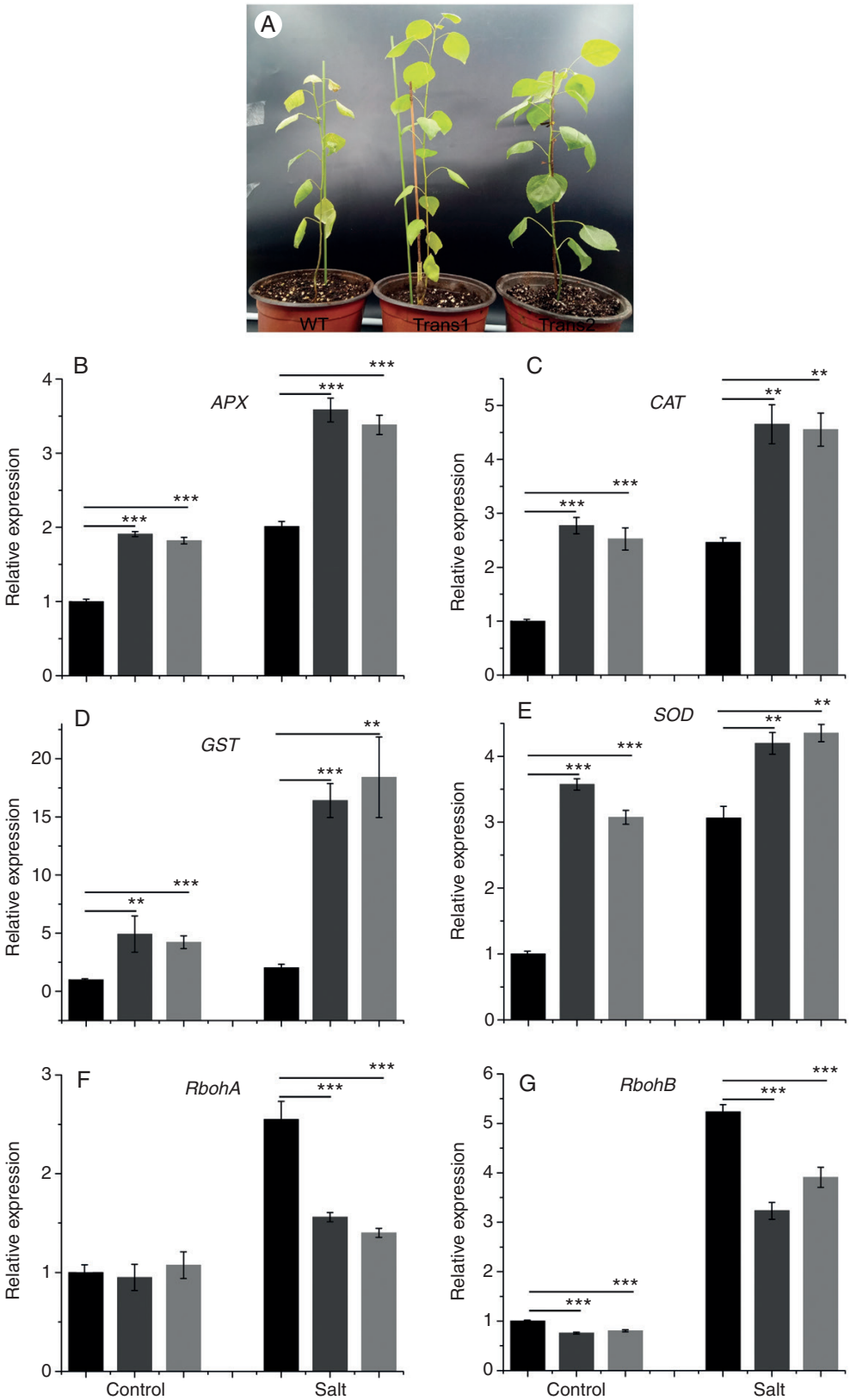

FIG. 11. Effect of salt stress on the (A) phenotype and transcript levels of (B) *APX*, (C) *CAT*, (D) *GST*, (E) *SOD*, (F) *RbohA*, and (G) *RbohB* of WT and transgenic poplar. Relative expression was calculated using *Actin* as an internal reference. WT leaves untreated with salt stress served as controls. Vertical bars are mean ± s.d. ($n = 3$). Black columns, WT; Trans1 and Trans2 represent two relatively independent transgenic lines, respectively, dark grey columns, Trans1; light grey columns, Trans2. Three independent experiments were performed. $^{**}P < 0.01$, $^{***}P < 0.001$.

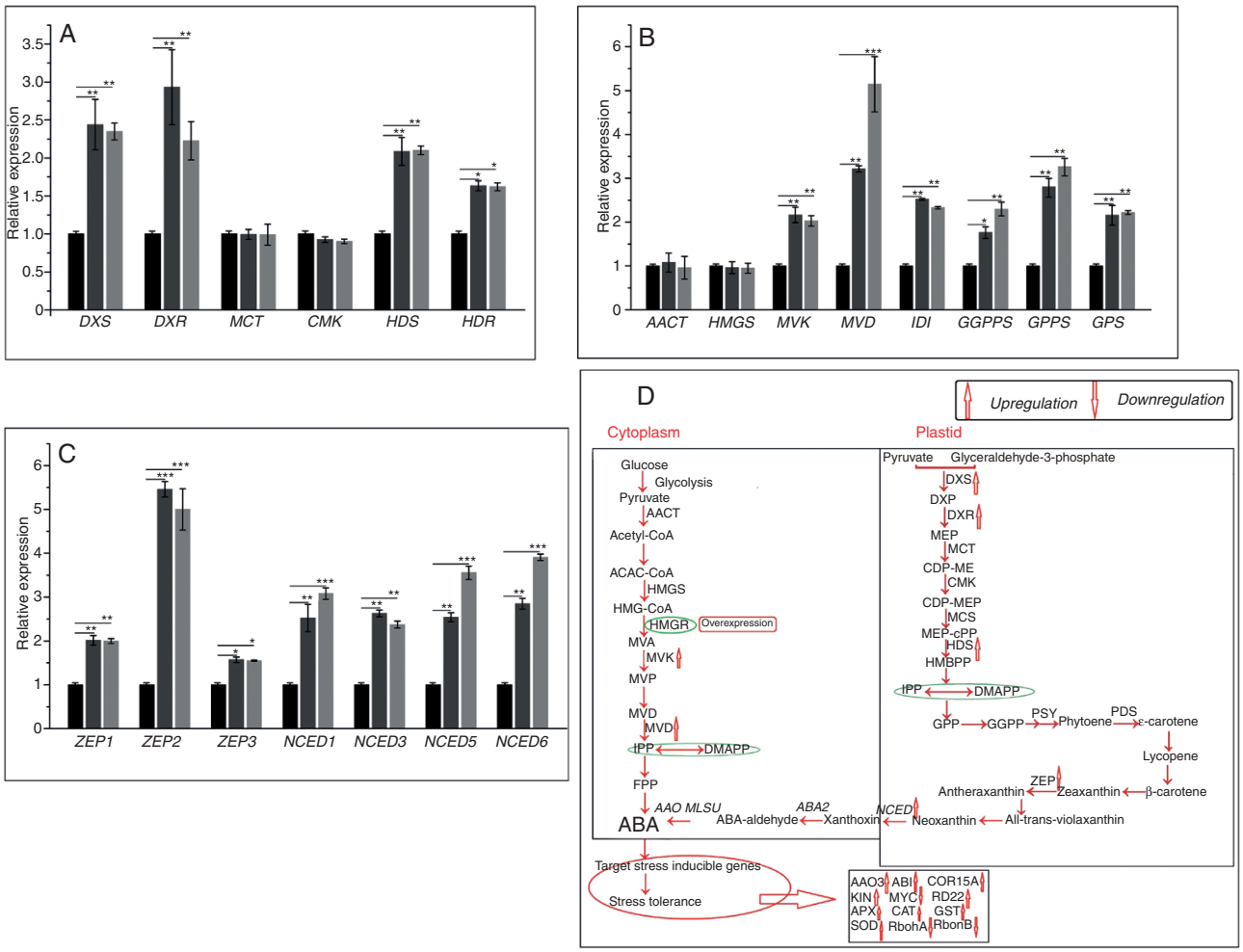

FIG. 12. Changes in WT and transgenic poplars in the transcript levels of (A) *DXS*, *DXR*, *MCT*, *CMK*, *HDS* and *HDR* (MEP-related genes); (B) *AACT*, *HMGS*, *MVK*, *MVD*, *IDI*, *GPS*, *GPPS* and *GGPPS* (mevalonate- and downstream-related genes); and (C) *ZEP1*, *ZEP2*, *ZEP3 NCED1*, *NCED3*, *NCED5* and *NCED6* (ABA-related genes). Black columns, WT; Trans1 and Trans2 represent two relatively independent transgenic lines, respectively, dark grey columns, Trans1; light grey columns, Trans2. (D) ABA-mediated signal transduction under drought and salt stress. Relative expression was calculated using *Actin* as an internal reference. Leaves treated with distilled water served as controls. Vertical bars are mean ± s.d. ($n = 3$). Three independent experiments were performed. $^{*}P < 0.05$, $^{**}P < 0.01$, $^{***}P < 0.001$.

in WT under salt stress (Fig. 11G) Under salt stress, the activities of SOD, POD and CAT and the proline content were higher in transgenic lines than in WT, and the MDA level was lower in transgenic lines (Fig. 10F–J). Therefore, *PtHMGR* modulates the expression of ROS scavenging-related genes, the activities of SOD, POD and CAT, and the MDA and proline contents of plant cells.

PtHMGR regulates the expression of MEP-, mevalonate- and ABA-related genes

Isoprenoid metabolites, such as cytokinin, gibberellin, ABA, chlorophyll and terpenoids, are important for maintaining plant growth and development and coping with environmental stresses (Mosquera *et al.*, 2016; Gupta *et al.*, 2017). Isoprene metabolites are mainly synthesized via the mevalonate and MEP pathways, in which the rate-limiting enzyme HMGR converts HMG-CoA to mevalonate. The transcript levels of 1-deoxy-D-xylulose5-phosphate synthase (*DXS*), 1-deoxy-D-xylulose5-phosphate reductoisomerase (*DXR*), 1-hydroxy-2-methyl-2-(*E*)-butenyl4-diphosphate synthase (*HDS*) and 1-hydroxy-2-methyl-2-(*E*)-butenyl4-diphosphate reductase (*HDR*) were increased significantly in transgenic lines, while those of acetoacetyl CoA thiolase (AACT), 2-*C*-methyl-D-erythritol 4-phosphate cytidylyltransferase (*MCT*) and 4-diphosphocytidyl-2-*C*-methyl-D-erythritol kinase (*CMK*) were not significantly different (Fig. 12A). In addition, the transcript levels of mevalonate kinase (*MVK*), mevalonate5-diphosphate decarboxylase (*MVD*), isopentenyl diphosphate isomerase (*IDI*), geranyl geranyl diphosphate synthase (*GGPPS*), geranyl diphosphate synthase (*GPPS*) and geranyl diphosphate (*GPS*) were increased significantly in transgenic lines (Fig. 12B), as were those of ABA-related genes (Fig. 12C). Therefore, PtHMGR regulates the expression of osmotic stress-related genes via the ABA signalling pathway to enhance tolerance of salt and drought stress (Fig. 12D).

DISCUSSION

The *HMGR*s, which encode the rate-limiting enzyme of the mevalonate pathway, have been isolated and cloned from *A. thaliana*, *O. sativa* and *Hevea brasiliensis* (Caelles *et al.*, 1989; Chye *et al.*, 1991; Nelson *et al.*, 1994). The open reading frame of *HMGR*s is 1–2 kb in length (most are ~1.7 kb) and encodes 500–600 amino acids. The amino acid sequences of most plant HMGRs have HMG-CoA- and NADPH-binding regions. The amino acid sequences of HMG-CoA-binding region 1 is EM(L) PVGYVQIP; the second amino acid in monocotyledonous plants (e.g. rice and maize) is leucine (L) and that in dicotyledons is methionine (M). HMG-CoA-binding region 2 has a conserved sequence (TTEGCLVA). The amino acid sequence of the NADPH-binding region is DAMGMNM or GTVGGGTQ. These residues are involved in substrate recognition and binding. In this study we cloned the 1767-bp (encoding 588 amino acids) *HMGR* gene from *P. trichocarpa*. PtHMGR contained HMGR-CoA (EMPVGYVQIP and TTEGCLVA)- and NADPH (DAMGMNM and GTVGGGTQ)-binding domains.

2*EpHMGR* and *CgHMGR* (Yechun *et al.*, 2007; Cao *et al.*, 2010) promote the biosynthesis of β-carotene in *E. coli*. Transfer of *TbHMGR1*, *TbHMGR2* and *TbHMGR3* enabled survival of *E. coli* defective in isoprene pyrophosphate synthesis through the endogenous MEP pathway. Indeed, these three HMGRs have similar activities and can restart the mevalonate pathway (Campos and Boronat, 1995). PtHMGR production in a prokaryotic system was unsuccessful. However, we obtained and purified PtHMGR protein in *P. pastoris* GS115. The PtHMGR then produced was capable of catalysing the formation of mevalonate from HMG-CoA and NADPH *in vitro*. The K_m value of PtHMGR for HMG-CoA was 7.91 ± 3.04. The HMG-CoA binding capacity of PtHMGR is similar to that of the corresponding proteins of *Z. mays* and *A. thaliana*, and stronger than that of *H. brasiliensis* (Wititsuwannakul *et al.*, 1990; Dale *et al.*, 2010).

3The expression level of *WsHMGR* increased in the order flower > root > fruit > stem > leaf and was higher in young than in mature leaves (Akhtar *et al.*, 2013). The transcript level of *CaHMGR* was high in stems, roots and leaves (Wang *et al.*, 2014). The expression of *PfHMGR* is reportedly high in roots and stems (Liang *et al.*, 2014). *ZmHMGR6* is highly expressed in seeds, *ZmHMGR5* is exclusively expressed in the endosperm of seeds, and soybean *GmHMGR4* is highly expressed during the late stage of seed development (Wei *et al.*, 2014). In the present study we found the highest expression accumulation in roots. In addition, previous studies demonstrated that the *HMGR* gene could respond to various treatments (Yukimune *et al.*, 1996; Wang *et al.*, 2014).

4In this study the transcript level of *PtHMGR* responded to ABA, JA, SA, NaCl, PEG_{6000} and H_2O_2, suggesting it has roles in the responses to various stresses. These findings will facilitate the breeding of salt- and drought-resistant poplar varieties.

5Drought induces osmotic stress in plants, while salt stress induces osmotic stress and ion toxicity (Ahuja *et al.*, 2010). The secondary effects of drought and salt stress on plants include oxidative stress, damage to membrane lipids, proteins and nucleic acids, and disruption of metabolism. Primary stress signals may induce cellular responses, but secondary stress signals are typically more important. Therefore, drought and salinity stress have specific signal transduction pathways, which can engage in cross-talk. Both drought and salt stress induce hyperosmotic signals, leading to the accumulation of ABA and a variety of responses in plants. In this study we observed that the expression levels of mevalonate- and MEP-related genes were increased in transgenic poplars. In addition, the transcript levels of ABA-related genes and ABA contents were increased in transgenic poplars (Supplementary Data Fig. S7). ABA is critical for the response of plants to abiotic stresses, including drought and salt (Zhu, 2000). The ABA signalling pathway consists of a subfamily of PP2Cs and three kinases, SnRK2-2/3/6, whose activity is controlled by the concentration of ABA. In the absence of ABA, the PYL receptor proteins do not interact with PP2Cs (ABI1, ABI2 and HAB1). The PP2Cs inactivate SnRK2 by phosphorylation, suppressing the expression of ABA-responsive genes. The serine subunit in the activation loop of SnRK2s was phosphorylated by PP2C (Ng *et al.*, 2011; Soon *et al.*, 2012) Above a threshold concentration, ABA binds to PYL receptors, which promotes its binding to the catalytic site of PP2Cs. The ABA–PYL complex inhibits PP2C kinase activity, resulting in release of SnRK2s. SnRK2 auto-phosphorylates and transmits ABA signals to downstream factors, which initiate the plant response to drought and salt stresses (Fujii *et al.*, 2009; Park *et al.*, 2009). In this study the transcript levels of ABA-responsive genes (including *AAO3*, *ABI*, *COR15A*, *KIN*, *MYB*, *MYC* and *RD22*) differed significantly between the transgenic and WT poplars after salt and drought stress. In addition, the roots of *PtHMGR*-overexpressing poplar seedlings developed rapidly, and the transgenic poplars had a high survival rate and enhanced tolerance of osmotic stress. The expression levels of genes related to ROS scavenging were higher in the *PtHMGR*-overexpressing (*PtHMGR-OE*) poplars under osmotic stress conditions, and the transcript levels of genes related to ROS formation were lower in transgenic poplars under osmotic stress conditions, which indicated that the *PtHMGR-OE* poplars could not only produce less ROS, but also produce more ROS scavengers under osmotic stress conditions. In addition, the activities of SOD, POD and CAT in transgenic poplars were higher than those in WT under normal or osmotic stress conditions. SOD, POD and CAT scavenge ROS and peroxide free radicals in plants (Kar *et al.*, 2011). Therefore, overexpression of *PtHMGR* maintains the stability of the ROS system in poplar.

Conclusions

We cloned *PtHMGR* from *P. trichocarpa* and constructed a phylogenetic tree based on the amino acid sequences of plant HMGRs. The function and evolution of plant *HMGR* genes were conserved, making *HMGR* useful as a reference for assessing relationships among species. Overexpression of *PtHMGR* promoted root development, increased the expression of genes related to ROS scavenging, decreased the expression of genes related to ROS formation and increased the activity of antioxidant enzymes in transgenic poplars, enhancing their tolerance of osmotic stress. In addition, overexpression of *PtHMGR* increased expression of the stress-related genes *KIN1*, *COR15* and *AAO3*, and decreased that of *ABI*, *MYB*, *MYC2* and *RD22*, enhancing the stress resistance of poplar.

SUPPLEMENTARY DATA

Supplementary data are available online at https://academic.oup.com/aob and consist of the following. Figure S1: samples were extracted from mature and young leaves, upper and lower stems, petioles and roots. Figure S2: nucleotide and deduced amino acid sequences of PtHMGR. Figure S3: amino acid sequence alignments of PtHMGR and other HMGRs. Figure S4: three-dimensional structure of PtHMGR, AtHMGR, NtHMGR, OsHMGR and ZmHMGR. Figure S5: construction of Michaelis equation for PtHMGR protein. Figure S6: identification of transgenic lines. Figure S7: HPLC-MS/MS analysis of the ABA content of WT and transgenic poplars. Table S1: primers used in this study.

FUNDING

This work was supported by the National Key Program on Transgenic Research (2018ZX08020002), the National Science Foundation of China (31570650) and the Priority Academic Program Development of Jiangsu Higher Education Institutions.

ACKNOWLEDGEMENTS

The authors declare no conflicts of interest.

LITERATURE CITED

Ahuja I, Vos RCHD, Bones AM, Hall RD. 2010. Plant molecular stress responses face climate change. *Trends in Plant Science* **15**: 664–674.

Akhtar N, Gupta P, Sangwan NS, *et al.* 2013. Cloning and functional characterization of 3-hydroxy-3-methylglutaryl coenzyme A reductase gene from *Withania somnifera*: an important medicinal plant. *Protoplasma* **250**: 613–622.

Caelles C, Ferrer A, Balcells L, Hegardt FG, Boronat A. 1989. Isolation and structural characterization of a cDNA encoding *Arabidopsis thaliana* 3-hydroxy-3-methylglutaryl coenzyme A reductase. *Plant Molecular Biology* **13**: 627–638.

Campos N, Boronat A. 1995. Targeting and topology in the membrane of plant 3-hydroxy-3-methylglutaryl coenzyme A reductase. *Plant Cell* **7**: 2163–2174.

Cao X, Zong Z, Ju X, *et al.* 2010. Molecular cloning, characterization and function analysis of the gene encoding HMG-CoA reductase from *Euphorbia pekinensis* Rupr. *Molecular Biology Reports* **37**: 1559–1567.

Caelles C, Ferrer A, Balcells L, Hegardt FG, Boronat A. 1989. Isolation and structural characterization of a cDNA encoding *Arabidopsis thaliana* 3-hydroxy-3-methylglutaryl coenzyme A reductase. *Plant Molecular Biology* **13**: 627–638.

Chaves MM, Maroco JP, Pereira JS. 2003. Understanding plant responses to drought—from genes to the whole plant. *Functional Plant Biology* **30**: 239–264

Choudhury FK, Rivero RM, Blumwald E, Mittler R. 2017. Reactive oxygen species, abiotic stress and stress combination. *Plant Journal* **90**: 856–867.

Christmann A, Hoffman T, Teplova I, Grill E, Müller A. 2005. Generation of active pools of abscisic acid revealed by *in vivo* imaging of water-stressed *Arabidopsis*. *Plant Physiology* **137**: 209–219.

Chye ML, Kush A, Tan CT, Chua NH. 1991. Characterization of cDNA and genomic clones encoding 3-hydroxy-3-methylglutaryl-coenzyme A reductase from *Hevea brasiliensis*. *Plant Molecular Biology* **16**: 567–577.

Dai Z, Cui G, Zhou SF, Zhang X, Huang L. 2011. Cloning and characterization of a novel 3-hydroxy-3-methylglutaryl coenzyme A reductase gene from *Salvia miltiorrhiza* involved in diterpenoid tanshinone accumulation. *Journal of Plant Physiology* **168**: 0–157.

Dale S, Arró M, Becerra B, *et al.* 2010. Bacterial expression of the catalytic domain of 3-hydroxy-3-methylglutaryl-CoA reductase (isoform HMGR1) from *Arabidopsis thaliana*, and its inactivation by phosphorylation at ser577 by *Brassica oleracea* 3-hydroxy-3-methylglutaryl-CoA reductase kinase. *European Journal of Biochemistry* **233**: 506–513.

Estevez JM, Cantero A, Reindl A, Reichler S, Leon P. 2001. 1-Deoxy-d-xylulose-5-phosphate synthase, a limiting enzyme for plastidic isoprenoid biosynthesis in plants. *Journal of Biological Chemistry* **276**: 22901–22909.

Finkelstein R. 2013. Abscisic acid synthesis and response. *The Arabidopsis Book* **11: e0166**.

Fujii H, Chinnusamy V, Rodrigues A, *et al.* 2009. *In vitro* reconstitution of an abscisic acid signalling pathway. *Nature* **462**: 660–664.

Gupta R, Singh A, Srivastava M, Singh V, Gupta MM, Pandey R. 2017. Microbial modulation of bacoside. A biosynthetic pathway and systemic defense mechanism in *Bacopa monnieri* under *Meloidogyne incognita* stress. *Science Reports* **7**: 41867.

Ha SH, Lee SW, Kim YM, Hwang YS. 2001. Molecular characterization of *hmg2* gene encoding a 3-hydroxy-methylglutaryl-CoA reductase in rice. *Molecules and Cells* **11**: 295–302.

Jing L, Li W, Rong D, Jinteng C, Kezhong Z, School LA. 2018. Analysis of key enzyme genes in carotenoid metabolism pathway of *Lilium* and cloning of *LOLCYB* gene. *Molecular Plant Breeding* **10**.

Kar RK. 2011. Plant responses to water stress: role of reactive oxygen species. *Plant Signaling & Behavior* **6**: 1741–1745.

Leivar P, Antolín-Llovera M, Arró M, Ferrer A, Boronat A, Campos N. 2011. Modulation of plant HMG-CoA reductase by protein phosphatase 2a. *Plant Signaling & Behavior* **6**: 1127–1131.

Liang Y, Jiang XM, Hu Q, *et al.* 2014. Cloning and characterization of 3-hydroxy-3-methylglutaryl-CoA reductase (HMGR) gene from *Paris fargesii* Franch. *Indian Journal of Biochemistry and Biophysics* **51**: 201–206.

Livak KJ, Schmittgen TD. 2001. Analysis of relative gene expression data using real-time quantitative PCR and the 2− ΔΔCT method. *Methods* **25**: 402–408.

Loreto F, Schnitzler JP. 2010. Abiotic stresses and induced BVOCs. *Trends in Plant Science* **15**: 154–166.

Loreto F, Dicke M, Schnitzler JP, Turlings TC. 2014. Plant volatiles and the environment. *Plant Cell & Environment* **37**: 1905–1908.

Maldonado-Mendoza IE, Burnett RJ, Nessler CL. 1992. Nucleotide sequence of a cDNA encoding 3-hydroxy-3-methylglutaryl coenzyme A reductase from *Catharanthus roseus*. *Plant Physiology* **100**: 1613–16.

Markus Lange B, Rujan T, Martin W, Croteau R. 2000. Isoprenoid biosynthesis: the evolution of two ancient and distinct pathways across genomes. *Proceedings of the National Academy of Sciences of the USA* **97**: 13172–13177.

Mithöfer A, Boland W. 2012. Plant defense against herbivores: chemical aspects. *Annual Review of Plant Biology* **63**: 431–450.

Miziorko HM. 2011. Enzymes of the mevalonate pathway of isoprenoid biosynthesis. *Archives of Biochemistry & Biophysics* **505**: 0–143.

Mosquera T, Alvarez MF, José M, *et al.* 2016. Targeted and untargeted approaches unravel novel candidate genes and diagnostic SNPs for quantitative resistance of the potato (*Solanum tuberosum* L.) to *Phytophthora infestans* causing the late blight disease. *PLoS ONE* **11**: e0156254.

Nelson AJ, Doerner PW, Zhu Q, Lamb CJ. 1994. Isolation of a monocot 3-hydroxy-3-methylglutaryl coenzyme a reductase gene that is elicitor-inducible. *Plant Molecular Biology* **25**: 401–412.

Ng LM, Soon FF, Zhou XE, *et al.* 2011. Structural basis for basal activity and autoactivation of abscisic acid (ABA) signaling SnRK2 kinases. *Proceedings of the National Academy of Sciences of the USA* **108**: 21259–21264.

Park SY, Fung P, Nishimura N, *et al.* 2009. Abscisic acid inhibits type 2C protein phosphatases via the PYR/PYL family of START proteins. *Science* **324**: 1068–1071.

Schwender J, Gemünden C, Lichtenthaler HK. 2001. Chlorophyta exclusively use the 1-deoxyxylulose 5-phosphate/2-c-methylerythritol 4-phosphate pathway for the biosynthesis of isoprenoids. *Planta* **212**: 416–423.

Seo M, Koshiba T. 2002. Complex regulation of ABA biosynthesis in plants. *Trends in Plant Science* **7**: 41–48.

Soon FF, Ng LM, Zhou XE, *et al.* 2012. Molecular mimicry regulates ABA signaling by SnRK2 kinases and PP2C phosphatases. *Science* **335**: 85–88.

Sun L, Sun Y, Zhang M, *et al.* 2012. Suppression of 9-cis-epoxycarotenoid dioxygenase, which encodes a key enzyme in abscisic acid biosynthesis, alters fruit texture in transgenic tomato. *Plant Physiology* **158**: 283–298.

Székely G, Ábrahám E, Cséplő A, *et al.* 2008. Duplicated *p5cs* genes of *Arabidopsis* play distinct roles in stress regulation and developmental control of proline biosynthesis. *Plant Journal* **53**: 18.

Tuskan GA, Difazio S, Jansson S, *et al.* 2006. The genome of black cottonwood, *Populus trichocarpa* (Torr. & Gray). *Science* **313**: 1596–1604.

Vickers CE, Gershenzon J, Lerdau MT, Loreto F. 2009. A unified mechanism of action for volatile isoprenoids in plant abiotic stress. *Nature Chemical Biology* **5**: 283–291.

Wang QJ, Zheng LP, Zhao PF, Zhao YL, Wang JW. 2014. Cloning and characterization of an elicitor-responsive gene encoding 3-hydroxy-3-methylglutaryl coenzyme A reductase involved in 20-hydroxyecdysone production in cell cultures of *Cyanotis arachnoidea*. *Plant Physiology and Biochemistry* **84**: 1–9.

Wei L, Wei L, Hengling W, *et al.* 2014. Species-specific expansion and molecular evolution of the 3-hydroxy-3-methylglutaryl coenzyme A reductase (HMGR) gene family in plants. *PLoS ONE* **9**: e94172.

Wititsuwannakul R, Wititsuwannakul D, Suwanmanee P. 1990. 3-Hydroxy-3-methylglutaryl coenzyme A reductase from the latex of *Hevea brasiliensis*. *Phytochemistry* **29**: 1401–1403.

Wu TS, Leu YL, Chan YY, *et al.* 1997. Tetranortriterpenoid insect antifeedants from *Severinia buxifolia*. *Phytochemistry* **45**: 1393–1398.

Xiong L, Schumaker KS, Zhu JK. 2002. Cell signaling during cold, drought, and salt stress. *Plant Cell* **14**: 165–183.

Xiuli HU, Zhang A, Zhang J, Jiang M. 2006. Abscisic acid is a key inducer of hydrogen peroxide production in leaves of maize plants exposed to water stress. *Plant & Cell Physiology* **47**:1484–1495.

Yechun W, Binhui G, Fei Z, Hongyan Y, Zhiqi M, Kexuan T. 2007. Molecular cloning and functional analysis of the gene encoding 3-hydroxy-3-methylglutaryl coenzyme A reductase from hazel (*Corylus avellana* L. Gasaway). *Journal of Biochemistry & Molecular Biology* **40**:861–869.

Yonekura-Sakakibara K, Saito K. 2009. Functional genomics for plant natural product biosynthesis. *Natural Product Reports* **26**: 1466–1487.

Yu F, Utsumi R. 2009. Diversity, regulation, and genetic manipulation of plant mono- and sesquiterpenoid biosynthesis. *Cellular and Molecular Life Sciences* **66**: 3043–3052.

Yukimune Y, Tabata H, Higashi Y, Hara Y. 1996. Methyl jasmonate-induced overproduction of paclitaxel and baccatin III in *Taxus* cell suspension cultures. *Nature Biotechnology* **14**: 1129–1132.

Zhang J, Movahedi A, Sang M, *et al.* 2017. Functional analyses of NDPK2 in *Populus trichocarpa*, and overexpression of *PtNDPK2*, enhances growth and tolerance to abiotic stresses in transgenic poplar. *Plant Physiology and Biochemistry* **117**: 61–74.

Zhang M, Leng P, Zhang G, Li X. 2009. Cloning and functional analysis of 9-cis-epoxycarotenoid dioxygenase (NCED) genes encoding a key enzyme during abscisic acid biosynthesis from peach and grape fruits. *Journal of Plant Physiology* **166**: 0–1252.

Zhu JK. 2000. Genetic analysis of plant salt tolerance using *Arabidopsis*. *Plant Physiology* **124**: 941–948.